Towards Sustainable Elastomers from the Grafting-Through Polymerization of Lactone-containing Polyester Macromonomers

*Lucie Fournier, Daniela M. Rivera Mirabal and Marc A. Hillmyer**

Department of Chemistry, University of Minnesota, Minneapolis, Minnesota 55455-0431, United States

*Corresponding author (hillmyer@umn.edu)

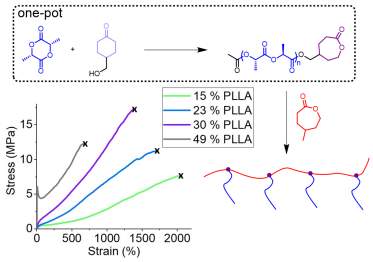

For Table of Contents use only

ABSTRACT. As the need for renewable and degradable alternative plastics grows, efforts have been made to develop biobased polymer architectures with tunable properties. We developed the synthesis of a new, biobased, and degradable graft copolymer using a grafting-through approach. A one-pot strategy was developed for the synthesis of telechelic poly(L-lactide) (PLLA) with a polymerizable lactone group at one chain end. Using mild conditions, the lactone functionalized polymer was obtained after three steps. Conditions were optimized and complete conversion was reached in each step. The polyesters were characterized by ^{1}H and ^{13}C nuclear magnetic resonance (NMR) spectroscopies, size exclusion chromatography (SEC), and matrix assisted laser desorption ionization - time of flight (MALDI-TOF) mass spectrometry. The macromonomers were then copolymerized with γ-methyl-ε-caprolactone (γMCL) to prepare fully aliphatic polyester graft copolymers. Using optimized conditions, a series of graft copolymers with graft length, backbone length and graft density variations were analyzed by NMR spectroscopy, SEC, thermogravimetric analysis (TGA) and differential scanning calorimetry (DSC). Mechanical properties were also evaluated, and the corresponding structure-property relationships were studied. Materials with highly tunable mechanical properties were obtained. One of the graft polymers with 30 wt% PLLA showed impressive elastomeric behavior with about 17 MPa stress at break and 1400 % strain at break, and a residual strain at 25 % after the 2nd cycle and 40 % after the 10th cycle. This study opens the door to the use of ring opening transesterification polymerization (ROTEP) for the synthesis of new fully biobased graft copolymers.

Introduction

The production and disposal of plastics that find myriad uses in our everyday lives, is still challenged with environmental problems that include the use of finite fossil starting materials and their common disposal in landfills. In 2019, about 368 million metric tons (Mt) of plastic were produced.[1] Despite growing efforts for a more sustainable world, only 3.8 Mt, or about 1 %, were biobased polymers.[2] There is still a need for sustainable polymers that are more competitive with commercial plastics from both economic and material properties perspectives. As new polymer architectures are developed, the 12 principles of green chemistry are important tools in the design and development of novel polymerization strategies, e.g., atom economy, solvent use and the mode of polymerization catalysis considerations.[3,4]

Thermoplastic elastomers (TPEs) combine the properties of elastomeric rubbers at room temperature and those of reprocessable and recyclable thermoplastics when heated.[5] To achieve these properties, typical TPEs contain two types of polymers, a glassy or semi-crystalline one (A) and a rubbery one (B). They can be arranged in an ABA triblock architecture with polystyrene (PS) as the A block and polyisoprene (PI) as the B block, for example.[6] TPEs have also been reported with graft architectures, B-*g*-A. For example, PI-*g*-PS, or polyisoprene chains decorated with PS grafts, materials exhibit "superelasticity", meaning they are characterized by high strains at break (up to 1400 % in that example) and a low residual strains, owing to a long PI backbone and high grafting density of PS chains.[7] Graft copolymers can be obtained using grafting-to, grafting-from and grafting-through methods. The grafting-through method offers control over the graft length, simplicity and versatility. Indeed, to enable a grafting-through approach, distinct chemistries have been used for the copolymerization of the macromonomer[8] with common examples being by atom transfer radical polymerization[9] or ring-opening metathesis polymerization.[10,11,12] Only few

examples of the use of ring opening transesterification polymerization (ROTEP) for the grafting-through copolymerization of a lactone-containing macromonomer have been reported; two relevant examples reported about two decades ago are: poly(ε-caprolactone)-*g*-poly(methylmethacrylate)[13] and poly(ε-caprolactone)-*g*-poly(ethylene oxide).[14]

Efforts to incorporate in more biobased components in TPEs have been reported, and in many of those, poly(L-lactide) (PLLA) was used as a semi-crystalline, hard (A) block. PLLA is an appealing polymer as it can be biodegradable under appropriate conditions and can be obtained from renewable resources such as corn or sugar beets.[15] For those reasons, PLLA has been used in TPEs because of its properties resembling those of polystyrene.[16] Specifically, graft polymers containing semi-crystalline PLLA have been reported with PLLA as the graft: polybutadiene-*g*-PLLA,[17,18] poly(γ-glutamic acid)-*g*-polylactide,[19] poly[n-butyl (meth)acrylate-*g*-lactic acid]s.[20] With the graft being a copolymer: polybutadiene-*g*-(1,3-trimethylene carbonate-*b*-LLA), (PB-*g*-(TMC-*b*-LLA), PB-*g*-(LLA-*ran*-TMC), PB-*g*-(LLA-*grad*-TMC),[21] poly[(n-butyl acrylate)-*co*-(2-hydroxyethyl acrylate)]-*g*-poly[(ε-decalactone)-*b*-(LLA)][22] and poly[(styrene-*alt*-N-hydroxyethylmaleimide)-*stat*-(styrene-*alt*-N-ethylmaleimide)]-*g*-poly[(γ-methyl-ε-caprolactone)-*b*-lactide]. In this last example, the microphase separated graft copolymers with P(γMCL)-*b*-PLA side chains, containing 20 wt% of rubbery poly(γ-methyl-ε-caprolactone) (P(γMCL)), showed delayed aging compared to pure PLA (which embrittled in less than 2 days), remaining ductile after 210 days at ambient conditions.[23] Also, PLLA has been grafted onto different types of materials: graphene oxide,[24,25] lignin,[26] chitosan,[27,28] chitin,[29] cellulose nanofibers[30] and cellulose acetate.[31,32] Examples of graft polymers with PLLA as the backbone have also been studied.[33] However, few examples of fully biobased synthetic copolymers with PLLA as the graft have been reported. One example is poly(β-myrcene)-*g*-poly(L-lactide) which showed a high stress at break, but with low strains at break

(<110 %).[34,35] We were thus interested in the synthesis of a fully biobased, compostable, aliphatic polyester graft TPEs with competitive elastomeric properties.

γ-Methyl-ε-caprolactone (γMCL) has been used as a soft block in TPEs, for example in triblocks[36] and star polymers with PLLA[37] end blocks which have shown very promising mechanical properties. γMCL can be synthesized from *p*-cresol which can be derived from lignin. Lundberg *et al*. reported a techno-economic study for its manufacture based on a two-step process leading to a reasonable cost estimate.[38] From a recent respirometry and cell viability study on γMCL and LLA copolymers, poly(γ-methyl-ε-caprolactone) (P(γMCL)) was shown to be compostable under industrial conditions.[39] For those reasons, P(γMCL) is a good candidate to be used as a graft copolymer backbone. In this work, we report the one-pot synthesis of a PLLA macromonomer with a lactone as one chain-end and its copolymerization with γMCL by ROTEP. Numerous graft copolymers were synthesized using this new approach with different backbone lengths, graft densities and graft lengths, and the effects of these structural changes on thermal and mechanical properties were studied.

Experimental Section

Materials. 4-hydroxycyclohexanone (purchased from Crysdot) and 4-(hydroxymethyl)cyclohexanone (purchased from Millipore Sigma) were dried over molecular sieves and distilled three times, put through three freeze-pump-thaw cycles and stored in the glovebox. L-Lactide was provided by Altasorb (a subsidiary of Ortec, Inc.). It was recrystallized three times in toluene, dried, and stored in the glovebox freezer. 1,8-Diazabicyclo[5.4.0]undec-7-ene, diphenyl phosphate, and benzyl alcohol were purchased from Millipore Sigma, stored in the glovebox under nitrogen and used as received. Acetic anhydride and acetic acid were purchased

from Fisher Scientific and used without further purification. Meta-chloroperoxybenzoic acid (purchased from Millipore Sigma) was stored in the freezer and used as received. γ-Methyl-ε-caprolactone was synthesized following literature procedure,[36] dried over calcium hydride, distilled 3 times, and put through three freeze-pump-thaw cycles before being stored in a glovebox. Cyclopentyl methyl ether (purchased from Millipore Sigma) was used without further purification under argon. Dichloromethane, tetrahydrofuran, and toluene were dried through a drying column purification system from JC Meyer and degassed through three freeze-pump-thaw cycles and were then stored in the glovebox.

Nuclear Magnetic Resonance (NMR) Spectroscopy. NMR spectra were collected on a Bruker Avance III 500 spectrometer operating at 500 MHz and samples were dissolved in $CDCl_3$.

Size Exclusion Chromatography (SEC). Mass-average molar mass, number-average molar mass, and molar mass dispersity were measured using an Agilent1100 series liquid chromatography instrument. Experiments were performed with three Phenomenex Phenogel-5 columns aligned in series with THF as the mobile phase or three Varian PLgel Mixed C Columns with chloroform as the mobile phase. A Wyatt Technology DAWN DSP MALLS detector and a Wyatt opt lab EX RI S11 detector were used to collect the chromatograms for the THF experiments and an HP1047A refractive index detector for the chloroform experiments. The dn/dc values were estimated with an "in-line" method that uses the total area of the RI signal for samples of a known concentration and assumes 100 % of the sample mass is recovered.

MALDI-TOF Mass Spectrometry. Matrix assisted laser desorption/ionization spectra were obtained using an AB Sciex 5800 MALDI TOF/TOF system, equipped with two-stage time of flight (TOF) analysis and an Opti-Beam™ on-axis Nd:YAG laser. All spectra were collected in positive ion and reflector operating modes. Sample spot preparation was as follows. A 20 mg/mL

solution in THF of trans-2-[3-(4-tert-butylphenyl)-2-methyl-2-propenylidene]malononitrile (DCTB) matrix and a 1 mg/mL solution in THF of potassium trifluoroacetate (KTFA) or lithium bromide positive ion salt were mixed 10:1, respectively, to prepare a stock matrix:salt solution. A 2 mg/mL polymer solution was prepared separately in THF. A 1 μL volume of the matrix:salt stock solution was pulled into a 10 μL syringe, followed by 0.5 μL of the prepared polymer solution. The 1.5 μL matrix/salt/polymer solution was hand-spotted onto a MALDI sample plate and air dried before analysis.

Thermogravimetric Analysis (TGA). Thermogravimetric analysis was performed on a TA Instruments Q500 Analyzer at a heating rate of 10 °C/min from room temperature to 550 °C under nitrogen atmosphere.

Differential Scanning Calorimetry (DSC). Differential scanning calorimetry was performed on a TA Instrument Q-1000. Experiments were performed using hermetically sealed aluminum pans. The T_g was estimated as the midpoint of the thermal transition in the curve of the second heating ramp at 5 °C/min, which was calculated using the instrument's TRIOS software.

Dog-bone preparation for tensile testing. Samples were placed between two Teflon sheets and melt-pressed (Wabash MPI Hydraulic Presse, Model G50H-19) at 180 °C for 8 min (first 3 min at 500 tons, then 5 min at 3000 tons) then quenched to room temperature using water cooling (~35 °C/min) through the hot press. After aging the samples for 24 h, dog-bone-shaped tensile bars were punched out, resulting in samples with approximately 0.5 mm thickness, 3 mm gauge width, and 16 mm gauge length.

Tensile Testing. Samples were tested to the point of break using Shimadzu Autograph AGS-X Tensile Tester and an extension rate of 50 mm/min. For hysteresis experiments, samples were tested for 10 cycles of 300 % strain at 50 mm/min.

Small-Angle X-Ray Scattering. Experiments were conducted at the DuPont-Northwestern Dow Collaborative Access Team (DND-CAT) synchrotron research center 5-ID-D beamline of Advanced Photon Source at Argonne National Laboratory.

Representative macromonomer synthesis. In a glovebox, 4-(hydroxymethyl)cyclohexanone (192 mg, 1.5 mmol, 1 eq.), L-lactide (15 g, 104 mmol, 69.4 eq.), DBU (10 μL, 0.069 mmol, 0.05 eq.) and 21 mL of dichloromethane were place in a Schlenk tube. The reaction mixture was sealed and stirred outside the glovebox at room temperature. After 10 min, an excess of acetic acid was added to stop the polymerization. Volatiles were removed under vacuum. Acetic anhydride (1.4 mL, 15 mmol, 10 eq.) was added and the reaction mixture was stirred at 135 °C. The reaction was cooled downed to room temperature after 30 min and subjected to reduced pressure to remove volatiles. Dichloromethane (10 mL) was added to dissolve the mixture. A solution of meta-chloroperbenzoic acid (1.35 g, 7.8 mmol, 4 eq.) in 20 mL of dichloromethane (previously dried over magnesium sulfate) was then added and the reaction was stirred at room temperature. After 10 h, the crude mixture was precipitated once into methanol and twice into hexane to yield the purified polymer as a white powder. **^{1}H NMR** (500 MHz, $CDCl_3$, δ ppm): 5.16 (q, 152.4 H, -OC*H*C=O), 4.33 and 4.18 (m, 2 H, OCH_2CH), 4.03 (m, 2 H, OCH_2CH_2), 2.74 and 2.62 (m, 2 H, CH_2CH_2CO), 2.12 (s, 3 H, CH_3CO), 1.98 (m, 5 H, CHCH_2CH_2 and CH_2C*H*CH_2), 1.58 (d, 463.1 H, CH_3CH). **^{13}C NMR** (125 MHz, $CDCl_3$, δ ppm): 176.2 (*C*OCH_2), 170.2 (*C*OCH_3), 169.7 (O*C*CH), 69.1 (*C*HCH_3), 68.5 (CH_2CH_2O), 67.2 (CH*C*H_2O), 39.7 (*C*HCH_2), 32.8 (*C*H_2CO), 32.2 (OCH_2*C*H_2CH), 24.8 (OCCH_2*C*H_2CH), 20.8 (*C*H_3CO), 16.8 (*C*H_3CH)

Representative grafting-through synthesis of P(γMCL)-*g*-P(LLA). In a glovebox, γ-methyl-ε-caprolactone (2.1 g, 16.4 mmol, 1858 eq.), PLLA macromonomer (11,100 g/mol, 900 mg, 0.083 mmol, 9.4 eq.), benzyl alcohol (0.92 μL, 0.0088 mmol, 1 eq.), diphenyl phosphate (41

mg, 0.16 mmol, 18.7 eq.) and 6 mL of toluene were placed in a Schlenk tube. The vessel was sealed and removed from the glovebox where the reaction mixture was stirred at 100 °C. After 10 h, the polymerization was stopped with excess triethylamine. The crude mixture was precipitated once into methanol and twice into hexane to yield the purified graft polymer as a white solid. **^{1}H NMR** (500 MHz, C_6D_6, δ ppm): 5.02 (q, 505.1 H, -OC*H*CO), 4.08 (m, 1258 H, -OCH_2CH$_2$), 3.46 (m, 2 H, HOCH_2), 2.18 (m, 1274 H, CH_2CO), 1.66 (m, 646 H, OCCH$_2$CH_2), 1.52 (m, 575 H, OCH$_2$CH_2), 1.44 (m, 1071 H, OCCH$_2$CH_2 and CH$_2$C*H*), 1.32 (d, 1381 H, OCHCH_3), 1.29 (m, OCH$_2$CH_2), 0.75 (d, 1867 H, CH$_2$CHCH_3).**^{13}C NMR** (125 MHz, C_6D_6, δ ppm): 173.0 (*C*OCH$_2$), 169.9 (*C*OCH), 69.4 (*C*HCO), 62.6 (*C*H$_2$O), 35.6 (*C*H$_2$CH$_2$O), 32.1 (*C*H$_2$CH$_2$CO), 32.0 (*C*H$_2$CO), 29.8 (*C*HCH$_2$), 19.1 (*C*H$_3$CHCH$_2$), 16.5 (*C*H$_3$CHO)

Results and Discussion

Macromonomer synthesis and characterization

To synthesize a telechelic polyester with a lactone as a chain-end, we used the following strategy: first the ROTEP of L-lactide was initiated by a hydroxy-containing cyclic ketone. Then acetic anhydride was used to end-cap the terminal -OH end group of PLLA to prohibit it from reacting in the next step and during the grafting-through ROTEP. Post-polymerization functionalization was then accomplished by oxidation of the ketone chain-end to the corresponding lactone. We explored methods to realize these three steps in a one-pot process to reduce solvent waste, time, energy and in a more economical manner (Figure 1).

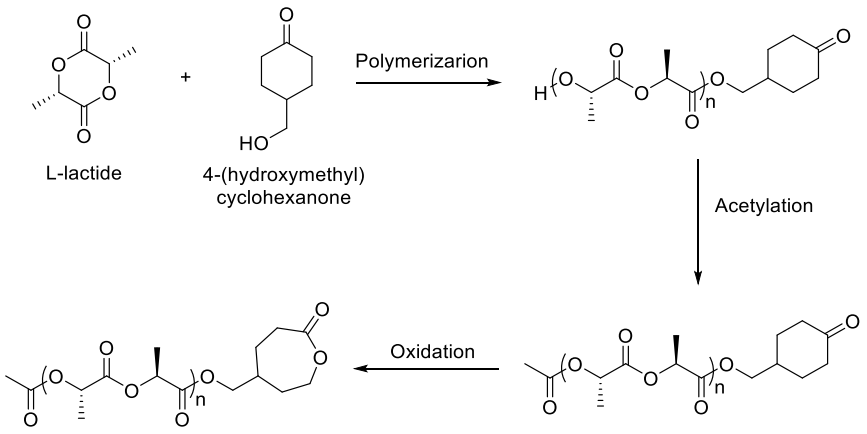

Figure 1. L-lactide macromonomer synthetic strategy.

The polymerization of L-lactide was first performed using a highly-active organocatalyst, 1,8-diazabicyclo[5.4.0]undec-7-ene (DBU),[40] with 4-(hydroxymethyl)cyclohexanone as the initiator. The second step is the addition of acetic anhydride, whose reaction with the hydroxy chain-end releases acetic acid, which deactivates the DBU and thus stops the polymerization. The oxidation was performed using meta-chloroperoxybenzoic acid (mCPBA),[41,42,43,44,45] which is highly efficient for Bayer-Villiger reactions on 6-member ring ketones.[36]

The steps were studied in concentrated solutions (to minimize the use of solvent) of different solvents. First, as previously reported,[46] under bulk conditions, the racemization of PLLA was problematic as it impacts the mechanical and thermal properties of the future grafts (

Table 1, entry 1). However, the acetylation step in bulk conditions, and with excess of acetic anhydride, reached complete conversion after only 30 min. Using dichloromethane, the polymerization was quite efficient, and no racemization could be observed by ^{1}H nuclear magnetic resonance (NMR). When the acetylation was performed at reflux in the polymerization mixture, the low boiling point of dichloromethane (i.e., the temperature of the reaction) resulted in poor

reactivity, and some hydroxyl end-groups were still present after two days at reflux. However, the following oxidation step was complete after 10 h (

Table 1, entry 2). To reduce the reaction time required for complete acetylation of the hydroxyl end-groups, higher boiling point solvents were tested. THF performed well for the polymerization, and showed better reactivity for the acetylation step, but was not an optimal solvent for the oxidation (

Table 1, entry 3). Toluene was very efficient for the acetylation, but the polymerization had to be performed at 70 °C to achieve an L-lactide at same level of concentration (5 M) than with dichloromethane. Racemization was observed, and THF was also a poor solvent for the oxidation step (

Table 1, entry 4). Cyclopentyl methyl ether (CPME) was then investigated as it is a green alternative to dichloromethane[47] and has a boiling point of 106 °C. L-lactide displayed poor solubility in CPME, even at 70 °C, more diluted conditions were thus used, giving high yields for both the polymerization and acetylation (at 50 °C) but poor activity for oxidation (

Table 1, entry 5 and 6).

Dichloromethane thus seemed the best choice for the polymerization and oxidation steps, but a higher temperature was required for an efficient acetylation. As such, the polymerization was first performed in dichloromethane, acetic acid was then added to stop the reaction, and volatiles (which could theoretically be recycled) were removed under reduced pressure. An excess of acetic anhydride, enough for the polymer to dissolve once heated, was added to the reaction mixture, which was then heated to 135 °C, leading to complete acetylation of the chain-ends after 30 min. Volatiles were again removed under reduced pressure and dichloromethane and mCPBA were added for the last step, which gave complete oxidation of the ketone after 10 h (

Table 1, entry 7). Taking the advantages of the polymerization in a solvent and the bulk acetylation, this strategy allowed the isolation of the purified telechelic PLLA macromonomer in three steps in less than 24 h, with complete conversion after each step, using a relatively small amount of recoverable and recyclable solvent and byproducts (i.e., acetic acid and excess acetic anhydride).

Table 1. One-pot poly(L-lactide) macromonomer synthesis optimization[a]

	Polymerization[a]						Acetylation[d]			Oxidation[e]		
Entry	Solvent	Conc. (M)	Temp. (°C)	Time (min)	Conv.[b] (%)	Rac.[b,c]	Temp. (°C)	Time (h)	Conv.[b] (%)	Conc. (M)	Time (h)	Conv.[b] (%)
1		8[f]	135	20	> 99	Yes	135	0.5	> 99	3[g]	10	> 99
2	CH_2Cl_2	5	r.t.	5	> 99	No	40	48	90	3	10	> 99
3	THF	5	50	30	> 99	No	66	24	95	4	96	57
4	Toluene	5	70	10	> 99	Yes	110	0.5	> 99	3	48	50
5	CPME	5	70	10	> 99	Yes	106	0.5	> 99	1	96	55
6	CPME	1	50	120	90	No	106	1	90	0.9	48	31
7[h]	CH_2Cl_2	5	r.t.	5	> 99	No	135	0.5	> 99	3.5	10	> 99

[a]0.5 mol% DBU, 70 eq. of LLA per initiator. [b]Determined by ^{1}H NMR spectroscopy. [c]Racemization of PLLA. [d]One-pot addition of 2 eq. of acetic anhydride at reflux. [e]One-pot addition of 4 eq. mCPBA in solution at room temperature. [f]Estimated using the density of L-lactide. [g]Dichloromethane was used to dissolve mCPBA. [h]Volatiles were evaporated between each step.

The macromonomers were characterized by ^{1}H NMR spectroscopy after polymerization, acetylation, and oxidation. We observed the complete disappearance of the original characteristic signals of the chain-end, and we were able to assign signals corresponding to the lactone chain-end from the spectrum of the purified macromonomer as detailed in Figure S4. Each step was also analyzed by size exclusion chromatography (SEC), and we observed that no change in apparent molar mass of the products had occurred after each of the post-polymerization functionalization steps (Figure 2).

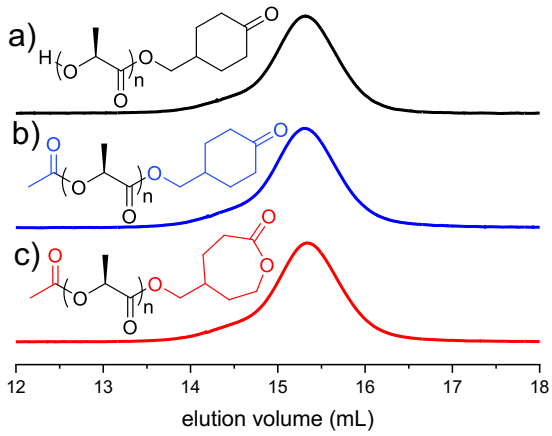

Figure 2. SEC spectra (chloroform as the eluent, RI detection). for each step of the one-pot L-lactide macromonomer synthesis (a) polymerization, top: M_n = 11,400 g/mol, M_w = 13,200 g/mol, M_w/M_n = 1.2; b) acetylation, middle: M_n = 11,400 g/mol, M_w = 13,200 g/mol, M_w/M_n = 1.2 c) oxidation, bottom: M_n = 11,400 g/mol, M_w = 13,200 g/mol, M_w/M_n = 1.2).

Matrix assisted laser desorption ionization - time of flight (MALDI-TOF) mass spectrometry experiments corroborated the success of each chain-end modification. Also, absolute masses of the products were confirmed; for example, the theoretical mass for the macromonomer with 16 lactide repeating units and the acetate and lactone chain-ends is 2497.8 g/mol and the observed mass from the MALDI-TOF spectrum is 2497.4 g/mol (Figure 3 and Figure S5).

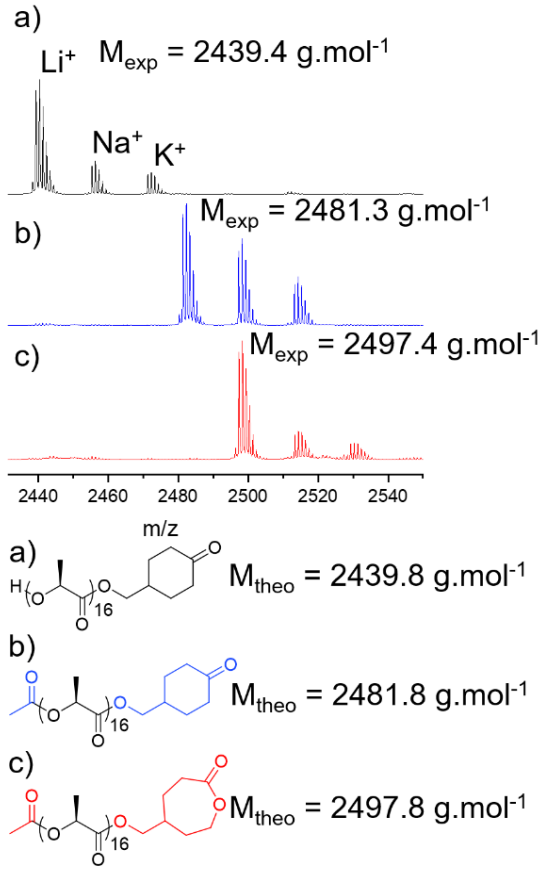

Figure 3. MALDI-TOF spectra using reflectron mode, of each step of the one-pot L-lactide macromonomer synthesis (a) polymerization b) acetylation c) oxidation), of zoomed-in area from 2400 to 2550 m/z (DCTB, LiBr). Calculations of the theoretical masses for n = 16 with a Li^+ ion are shown. Signals of polymers with Na^+ and K^+ ions from impurities were also observed.

PLLA macromonomers with molar masses ranging from 3 to 14 kg/mol were obtained with good control over the polymerization and complete conversion for the chain-end functionalization steps

(

Table 2, Figure S6), and were used for the grafting-through copolymerization with γMCL.

Table 2. Macromonomer synthesized of different molar masses[a]

Entry	$M_{n,\,theo}$ (g/mol)	$M_{n,\,NMR}$[b] (g/mol)	$M_{w,\,SEC\ THF\ LS}$[c] (g/mol)	M_w/M_n[c], SEC THF LS
1	2,300	2,900	3,000	1.3
2	6,000	7,100	7,900	1.2
3	10,200	11,100	11,300	1.2
4	11,800	14,000	13,800	1.2

[a]Synthesized from the optimized one-pot strategy [b]Determined by ^{1}H NMR spectroscopy [c]Calculated from THF SEC, 25 °C, light scattering detection.

Grafting-through copolymerization

When we first studied the optimization of the grafting-through process, a different macromonomer than the one described above was used; one synthesized with 4-hydroxycyclohexanone as the initiator (m=0, Scheme 1). However, using this macromonomer led to its intramolecular transesterification during grafting-through ROTEP (mechanism and details can be found in Figures S9-11), as previously identified in small molecule studies.[48] The intramolecular transesterification leads to a higher percentage of free (unincorporated) PLLA, and thus prevents a good control of the copolymerization. We characterized the level of free PLLA macromonomer in each sample as estimated by SEC analysis with light scattering detection. To overcome this problem, 4-(hydroxymethyl)cyclohexanone was used (as described above) to increase the distance between the two ester bonds and thus reduce the likelihood of intramolecular transesterification (m = 1, Scheme 1). Comparing the grafting-through polymerizations from these

two macromonomers clearly showed the elimination of intramolecular transesterification in the case of the m = 1 macromonomer (Table 3, entries 1-3 and Figure S12). Indeed, no residual macromonomer (or anything at the same elution volume) was observed at high conversion by SEC (Table 3, entry 3). We thus posit that all the lactone-end functionalized macromonomer was incorporated into the graft copolymer in that example.

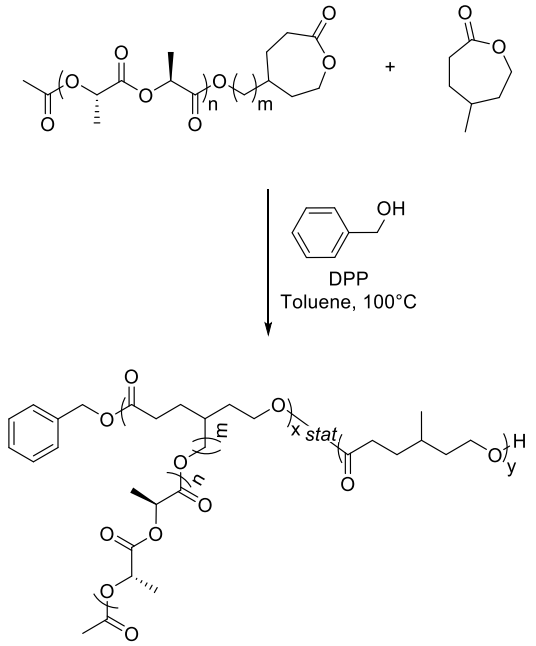

Scheme 1. Graft copolymer (P(γMCL)-*g*-PLLA) synthesis.

For the grafting-through polymerization we chose diphenyl phosphate (DPP) as the polymerization catalyst given its established reactivity in γMCL ROTEP[49] and poor reactivity towards lactide polymerization.[50] This difference in reactivity helps to mitigate transesterification between the growing P(γMCL) chains and the PLLA macromonomer repeat units or PLLA grafts. Indeed, using tin octanoate or titanium isopropoxide as catalysts resulted in transesterification as determined by SEC analysis. Using other common organocatalysts, such as 1,5,7-Triazabicyclo[4.4.0]dec-5-ene (which is highly active for LLA polymerization but is less active for

caprolactone polymerization), 37 would likely lead to transesterification of the PLLA chain prior to incorporation of the macromonomer and γMCL.

The grafting conditions were optimized through exploration of different temperatures, initiator loadings and concentrations (Table 3). A grafting-through copolymerization was performed at 135 °C with an initial monomer concentration of 2.5 M, after 9 h a polymer of 140 kg/mol (calculated by NMR spectroscopy) was obtained (Table 3, entry 3). The SEC data revealed a shoulder in the distribution at high molar mass, likely due to undesired transesterification. Under the same conditions but with a smaller amount of initiator, a higher theoretical value was targeted, however, the copolymer molar mass was not impacted (Table 3, entry 4). Other conditions were investigated to find the right equilibrium between a good reactivity and avoiding transesterification, and thus to have more control over the copolymerization. A reaction temperature of 100 °C was found to be, all things considered, most efficient to achieve polymers close to the theoretical molar mass and gave higher levels of incorporation of the macromonomer into the graft copolymer (Table 3, entries 5–8 and Figure 4). Conditions with a lower concentration did not result in better control (higher free PLLA contents, lower molar masses) of the copolymerization, even at high conversion (Table 3, entries 9-10 and Figure S13). Despite the optimization, the experimental molar masses of the resultant graft copolymers are about half of the theoretical values, and this can be explained by limitations associated with the catalyst (regarding the turnover number) and by incomplete incorporation of PLLA macromonomer in some cases, especially for high PLLA loadings. Nonetheless, the molar masses were high (some higher than for PLLA-*b*-P(γMCL)-*b*-PLLA triblocks),[36] and the most control and the highest graft/chain ratios were observed using 100 °C and 2.5 M initial monomer concentration, and thus these conditions were used for the balance of the study.

Table 3. Optimization of the grafting-through ROTEP[a]

Entry	m	Conc.[b] (M)	Temp (°C)	Time (h)	Conv.$_{\gamma MCL}$[c] (%)	$M_{n,\,theo}$ (kg/mol)	wt% Free PLLA[d,e]	wt% PLLA[c,d]	$M_{n,\,NMR}$[c,d] (kg/mol)	grafts/ chain[c,d]	$M_{w,\,SEC\ THF\ LS}$[d] (kg/mol)	M_w/M_n[d], $_{SEC\ THF\ LS}$
1	0	2.5	135	6	99	343	14	17	51	1.0	96	1.5
2	1	2.5	135	7.5	69	270	12	19	208	7.4	153	1.8
3	1	2.5	135	9	95	328	0	28	140	4.4	120	1.9
4	1	2.5	135	8	75	569	13	20	116	4.5	134	1.8
5	1	2.5	135	10	90	317	12	33	101	2.1	99	1.5
6	1	2.5	120	8	96	336	11	33	85	1.9	106	1.4
7	1	2.5	100	21	98	340	5.6	30	180	4.1	161	1.6
8	1	2.5	80	28	95	329	9	30	91	1.9	149	1.6
9	1	1	100	28	87	303	11	33	58	1.3	80	1.3
10	1	1	100	48	93	324	7.5	30	96	2.1	131	1.5

[a]With macromonomers of approximately 10 kg/mol, a starting a weight mixture of PLLA/PMCL of 30/70, with 1 mol% DPP in toluene. [b]Initial concentrations of monomers in toluene. [c]Determined by ^{1}H NMR spectroscopy. [d]Calculated from THF SEC, 25 °C, light scattering detected. [e]Unreacted macromonomer quantifiable on the SEC data of the pure copolymer.

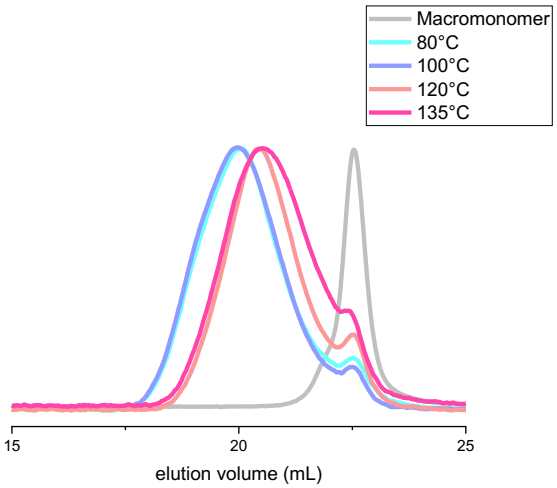

Figure 4. SEC data (THF as the eluant, RI detection) for the product graft copolymers synthesized at different temperatures (Table 3, entries 5-8).

To understand the grafting-through copolymerization statistics, we studied the kinetics of the copolymerization. Unfortunately, with the m = 1 macromonomer we were unable to determine the conversion of the macromonomer by ^{1}H NMR spectroscopy because of overlapping signals corresponding to CH_2 in α position to an oxygen atom. However, using the m = 0 macromonomer, some characteristic signals of the lactone chain-end of the macromonomer were identifiable. The reactivity ratio following the BSL non-terminal model were calculated for a copolymerization with 30 % PLLA macromonomer (m = 0, M_n = 10,200 g/mol), $r_{macromonomer}$ = 1.74 ± 0.25, $r_{\gamma MCL}$ = 0.71 ± 0.07; $r_{macromonomer}$ x $r_{\gamma MCL}$ = 1.23 ± 0.21 (Figures S14 and S15).[51] These results indicate a near-random structure for the graft copolymers but with a slight gradient. Interestingly, our data suggest a higher reactivity ratio for the macromonomer as compared to the γMCL under these conditions. We assume that m = 0 and m = 1 macromonomer have similar copolymerization behavior as their chemical structures are similar.

Four m = 1 macromonomer samples were used in the synthesis of a library of copolymers of different backbone length, graft density (the number of repeat units from the macromonomer for every 100 repeating units in the graft backbone) and PLLA content (Table S1). The graft copolymers we prepared were named as follow: $P(\gamma MCL)_x$-g_y-$P(LLA)_z$, where x is the average number of γMCL repeating units in the backbone, y is the average number of PLLA grafts along the backbone and z the average number of PLLA repeating units per graft. The dispersity of all the graft copolymers ranged from about 1.3 to 1.9, and the molar masses ranged from 46 to 165 kg/mol. The free PLLA percentages are mostly below 10 wt% except for reactions with a very high macromonomer feed (> 80 wt%). The higher the molar mass of the macromonomer, the more lactone terminated PLLA (referred in the tables as "free PLLA") was not incorporated in the graft copolymers. This result indicates that, with higher molar mass macromonomers, the graft copolymers may have more of a gradient structure, with the macromonomer having somewhat lower reactivity at the higher targeted and realized molar masses.

Thermal and mechanical properties

To understand the structure-property relationships in the graft copolymers, we studied the impact of graft length, fraction of PLLA, backbone length and graft density on the thermal and tensile properties (Table 4). The degradation temperatures ($T_{deg\ 5\%}$), defined here as the temperature at 5 % mass loss in the sample, ranged from 330–354 °C (Figure S16). Those are comparable to P(γMCL) degradation temperature (~350 °C)[49] but higher than those reported for PLLA (~290 °C).[52] This observation is consistent with previous reports that showed the end-capping of the alcohol chain-end by acetic anhydride stabilizes PLLA toward thermal degradation.[53,54] For most copolymers, differential scanning calorimetry (DSC) analysis showed two glass transition temperatures (T_g), around the T_g of PLLA (46 °C) and P(γMCL) (–58 °C) consistent with microphase separation of

these components (Figure S17). For copolymers with a PLLA content of 79 wt% and higher, only one T_g (≈ 29 °C) was observed, probably due to the low P(γMCL) content.

From the DSC measurements, percent PLLA crystallinity (%C) was calculated. The level of PLLA crystallinity was not clearly correlated with other parameters. The small-angle X-ray scattering (SAXS) data for the graft copolymer P(γMCL)$_{738}$-$g_{3.1}$-P(LLA)$_{49}$ were also acquired. At room temperature, a single broad peak at $q^* = 0.22$ nm^{-1} and thus a principal domain spacing of 28 nm was observed. When the material was heated to 175 °C, above its T_m, the peak was still evident. Thus, we conclude microphase separation still occurs in the melt state at 175 °C. Using an equation developed for PLLA-*b*-P(γMCL)-*b*-PLLA triblocks,[36] the segregation strength, χN, was estimated to be 68 at 175 °C.[55,56] The copolymer sample was then cooled down to room temperature and the scattering pattern prior to heating was recovered, suggesting that heating and cooling through the PLLA crystallization temperature (T_c of the graft copolymers samples are between 97 and 110 °C) did not disrupt the microphase separation and even allowed for enhanced organization of the domains (Figure S18). SAXS experiments were also conducted on a subset of graft polymers with varying PLLA content and graft density at fixed graft length. The SAXS data from these samples gave comparable principal domain spacings (d ≈ 25 nm) between 23 and 49 wt% PLLA, a higher domain spacing for 15 wt% PLLA (d ≈ 30 nm) and a lower one at 79 wt% PLLA (d ≈ 17 nm) (Figure S19). Meanwhile, comparing other set of data with various graft lengths, showed that the longer the graft, the higher the interdomain spacing; this is true even with the change in graft length being accompanied by a change in PLLA content (Figure S20) or graft density (Figure S21). Based on the lack of clear, sharp higher order reflections in the SAXS data, we conclude that the graft copolymers do not adopt well organized structures, especially for the polymers with a high grafting density.[57] This has been explained by the fact that high molar masses in graft copolymers, high

segregation strengths, as well as high graft density, may hinder the ability of the material to reach equilibrium morphologies. However, robust mechanical properties can be achieved without well-ordered microphase separation behavior.[6]

Table 4. Properties of different P(γMCL)-*g*-PLLA[a]

Entry	wt% tot. PLLA[b,c]	wt% Free PLLA[b]	Graft density[d] (%)	$M_{w,\ \text{SEC THF LS}}$[b] (kg/mol)	M_w/M_n[b], SEC THF LS	$T_{deg\ 5\%}$ (°C)[c]	T_g (°C)[e]	T_m (°C)[e]	%C[f]	E (MPa)[g]	σ_B (MPa)[g]	ε_B (%)[g]	U_T (MJ/m^3)[g]
$P(\gamma MCL)_{649}$-$g_{3.0}$-$P(LLA)_{20}$	9.4	0	0.46	100	1.7	345	-60/48	132	8.3	0.7	2.0	1670	2000
$P(\gamma MCL)_{1201}$-$g_{2.4}$-$P(LLA)_{49}$	14.9	5.6	0.20	152	1.8	340	-55/10	153	16	1.5	7.6	2040	7000
$P(\gamma MCL)_{1090}$-$g_{1.2}$-$P(LLA)_{76}$	13.7	5.5	0.11	133	1.5	349	-61/40	155	3.1	0.7	2.9	2170	3200
$P(\gamma MCL)_{738}$-$g_{3.1}$-$P(LLA)_{49}$	22.9	4.8	0.42	149	1.7	354	-60/36	150	11	1.6	11.2	1700	9800
$P(\gamma MCL)_{309}$-$g_{4.2}$-$P(LLA)_{20}$	26.7	4.3	1.35	55	1.6	342	-60/22	131	48	2.2	1.7	550	900
$P(\gamma MCL)_{420}$-$g_{6.4}$-$P(LLA)_{20}$	28.1	3.3	1.52	46	1.9	348	-58/49	134	39	3.1	6.2	1570	6300
$P(\gamma MCL)_{464}$-$g_{2.6}$-$P(LLA)_{49}$	29.9	7.8	0.57	88	1.6	348	-58/37	151	22	4.5	15.8	1330	10900
$P(\gamma MCL)_{779}$-$g_{4.5}$-$P(LLA)_{49}$	29.6	6.8	0.58	160	1.8	340	-58/39	150	8.9	3.8	14.4	1220	8500
$P(\gamma MCL)_{883}$-$g_{4.6}$-$P(LLA)_{49}$	29.5	9.3	0.52	163	1.8	340	-58/45	150	3.6	4.0	17.3	1380	11400
$P(\gamma MCL)_{393}$-$g_{2.2}$-$P(LLA)_{49}$	29.8	7.8	0.56	77	1.6	342	-60/30	142	60	4.4	5.2	1020	3500
$P(\gamma MCL)_{1048}$-$g_{4.1}$-$P(LLA)_{77}$	29.5	5.6	0.39	161	1.6	354	-60/31	153	13	2.7	10.3	750	3800
$P(\gamma MCL)_{487}$-$g_{1.1}$-$P(LLA)_{97}$	31.5	15	0.22	91	1.6	342	-60/38	156	4.7	3.9	7.5	710	3000
$P(\gamma MCL)_{726}$-$g_{2.9}$-$P(LLA)_{76}$	32	9.2	0.39	167	1.7	340	-59/38	155	1.9	5.7	13.1	1070	7400
$P(\gamma MCL)_{551}$-$g_{1.9}$-$P(LLA)_{97}$	37.7	15	0.34	162	1.6	337	-60/44	156	12	35	8.8	580	3400
$P(\gamma MCL)_{397}$-$g_{4.9}$-$P(LLA)_{49}$	48.8	14	1.2	162	1.8	342	-58/42	154	52	148	12.1	670	5100
$P(\gamma MCL)_{477}$-$g_{4.5}$-$P(LLA)_{76}$	51.3	12	0.94	165	1.6	340	-58/53	157	3.0	127	13.0	460	5200
$P(\gamma MCL)_{312}$-$g_{15.5}$-$P(LLA)_{49}$	78.5	20	5.0	99	1.4	330	28	155	50.0	42	1.7	4	3
$P(\gamma MCL)_{235}$-$g_{22.1}$-$P(LLA)_{49}$	88.6	29	14.0	157	1.7	332	29	158	55				

[a]Prepared using 1 mol% DPP at 100 °C, 2.5 M in toluene (Table S1) [b]Calculated from THF SEC, 25 °C, light scattering detected [c]Determined by ^{1}H NMR spectroscopy [c]Determined by TGA analysis at a heating rate of 10 °C min^{-1} [d]Percent of repeat units from the macromonomer for a 100 repeating units in the graft backbone [e]Determined on second heating cycle at a rate of 10 °C min^{-1} in a DSC analysis [f]Calculated (%C = ΔH_m / (ΔH_m^{∞} * wt%$_{PPLA}$)) from the second heating cycle at a rate of 10 °C min^{-1} (cooling at 5 °C min^{-1}) in a DSC analysis. [g]Determined from tensile testing to the break point of 4 samples extended at 50 mm.min^{-1}, a representative set of data was selected.

The mechanical properties of various graft architectures were studied by uniaxial tensile testing. As explained in the Introduction, using semi-crystalline PLLA hard block behavior is important to achieve high-performance thermoplastic elastomers. Indeed, using an amorphous, atactic PLA macromonomer resulted in a graft copolymer with considerably lower stress at break than a comparable PLLA graft copolymer (Figure S22). We first explored the impact of backbone length on the tensile behavior while other parameters (i.e., graft length, wt% PLLA and thus graft density) were kept relatively constant. At overall molar masses less than about 50 kg/mol, stresses at break were generally lower than 6 MPa; overall molar masses of 59 kg/mol or higher gave stresses at break greater than 14 MPa and strains at break higher than 1200 %. For molar masses between 59 and 133 kg/mol the backbone length, at constant graft density and thus constant PLLA content, had little impact on the tensile data in general (Figure 5 and S23).

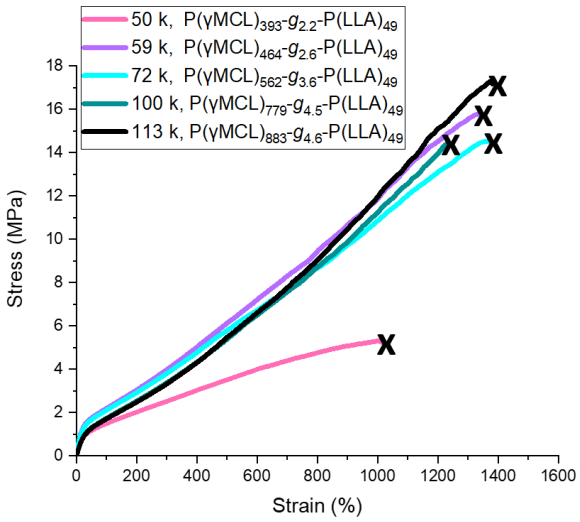

Figure 5. Representative stress–strain curves (of 4 samples extended at 50 mm.min^{-1}) for P(γMCL)-*g*-P(LLA) for different backbone length at approximately 30 wt% PLLA and a low graft density ≈ 0.6 %.

In a P(γMCL)-*g*-PLLA molecules with moderate to low grafting densities, there are two P(γMCL) blocks at the chain-ends, and several P(γMCL) bridging blocks between adjacent

PLLA grafts (Figure 6). Those elastically effective P(γMCL) segments bridge microphase separated PLLA domains, and consequently are kept in place by the PLLA glassy, semi-crystalline domains. A higher ratios of well-entangled P(γMCL) (M_e = 2.8 kg mol^{-1})[36] a higher bridging block to dangling end-block ratio is expected to give more desirable tensile properties.[58] Inherently, by changing the backbone length while keeping a constant graft density, the number of grafts per chain is impacted (here, from 2 to 5 grafts/chain, for the 50 kg/mol ($P(\gamma MCL)_{393}$-$g_{2.2}$-$P(LLA)_{49}$) and 113 kg/mol ($P(\gamma MCL)_{883}$-$g_{4.6}$-$P(LLA)_{49}$) samples, respectively). This could explain the improved tensile behavior for backbones with molar masses over 59 kg/mol (3 grafts/chain, $P(\gamma MCL)_{464}$-$g_{2.6}$-$P(LLA)_{49}$) as compared to copolymers with backbones at 50 kg/mol or less.

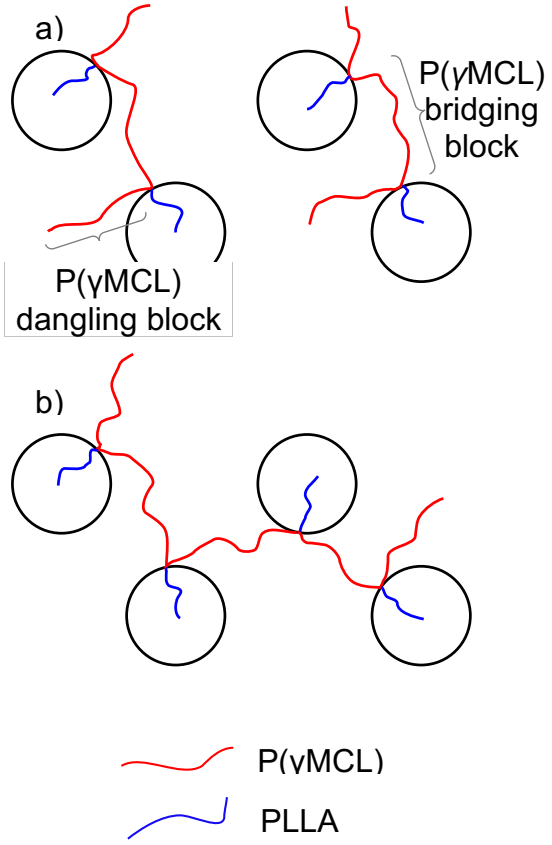

Figure 6. Schematic diagram showing P(γMCL) backbone with a (a) low grafting density; (b) high grafting density and the connections to the associated microphase separated PLLA domains.

The impacts of the (i) graft length, (ii) graft density, and (iii) PLLA content on tensile behavior in samples with similar backbone molar masses were next explored. Changing one of those parameters inherently impacts another, but it is possible to keep the third constant. First, we studied the impact of varying PLLA content by changing the graft density but keeping the graft length fixed (7.1 kg/mol) (Figure 7a)). As expected, the more PLLA, the higher the stress at break and the more plastic-like behavior. Above 50 wt% PLLA, these copolymers were brittle (Figure S23). At 15 wt% PLLA, the material displays a remarkable strain at break of 2000 %. At 30 wt% PLLA elongations at break of 1400 % with the highest stress at break value (17 MPa) was observed, those values are closed to the ones reported for PI-g-PS.[7] As previously described, the interdomain spacing was only slightly impacted when the PLLA content was varied between 15 and 49 wt%. However, the average molar mass of P(γMCL) segments decreases significantly (going from around 60 kg/mol for 15 wt% PLLA to only 10 kg/mol for 49 wt% PLLA) as the graft density changes. At about the same interdomain space, polymers with a lower PLLA content have longer P(γMCL) and more entangled segments between adjacent PLLA grafts (Figure 6), leading to superior elastomeric behavior. Consistently with the observations made for samples with different backbone lengths, the more PLLA grafts in the copolymers, the higher the stresses at break.

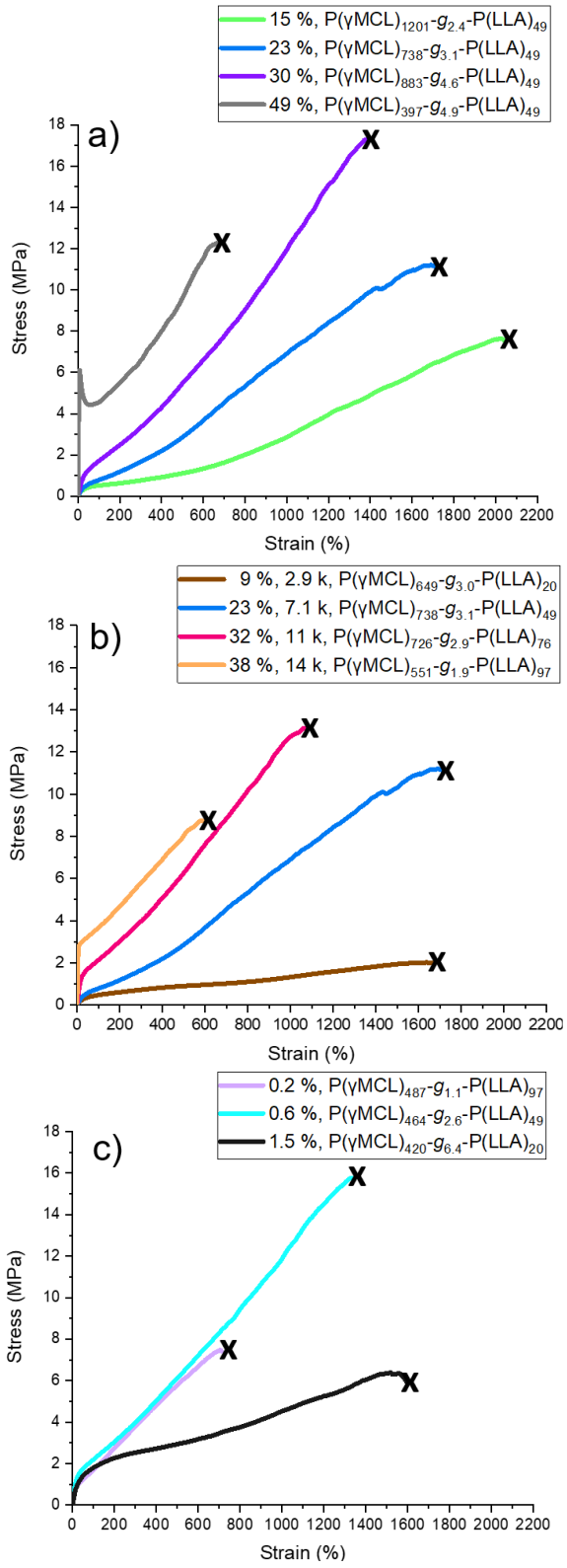

Figure 7. Representative stress–strain curves of 4 samples extended at 50 mm.min^{-1}, x represents break point, (a) for different PLLA content in the graft copolymers (15, 23, 30, and 49 wt%) by varying graft density (0.20, 0.42, 0.52 and 1.2 %, respectively), at fixed graft length

(7.1 kg/mol), (b) for different PLLA content (9, 23, 32, and 38 wt%) by varying graft length (2.9, 7.1, 11, and 14 kg/mol), at fixed graft density (0.4 ± 0.06 %), (c) for different graft density (0.2, 0.6, and 1.5 %) and graft length (2.9, 7.1, and 14 kg/mol, respectively), at fixed PLLA content (30 wt%).

Next, we studied the influence of PLLA content on tensile properties by varying the graft length instead of the graft density (Figure 7b)). The polymers with 7 kg/mol and 11 kg/mol PLLA grafts showed the most promising results, with stresses at break higher than 10 MPa and strains at break higher than 1000 %. The copolymer with 7 kg/mol PLLA grafts shows the lowest residual strain, 20 % after the 2nd cycle and 30 % after the 10th cycle, compared to 35 % and 50 % respectively, for the copolymer with 11 kg/mol grafts (Figure 8). However, the copolymer synthesized from the 14 kg/mol macromonomer exhibits a lower stress at break of only 8.8 MPa. This sample has a small number of grafts per chain (2, when the other graft copolymers have 3), and the P(γMCL) thus bridges fewer PLLA domains, resulting in lower strength, as shown for the backbone length study (Figure 6).

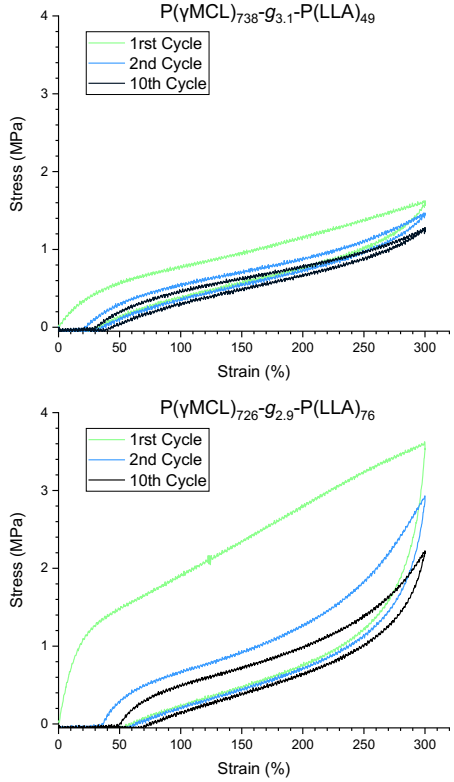

Figure 8. Hysteresis of P(γMCL)-*g*-PLLA for different PLLA content by varying graft length, at fixed graft density (0.4 ± 0.06 %) of 10 cycles of 300 % strain at 50 mm.min^{-1}.

As discussed previously, the graft copolymers contain a low level of "free PLLA", i.e., unreacted macromonomers. To determine the impact of the PLLA homopolymer on the tensile properties, we prepared blended samples (by dissolving them together in solvent and then drying them) from P(γMCL)$_{1201}$-g$_{2.4}$-P(LLA)$_{49}$ (containing an initially low free PLLA content of 5.6 wt%) and a variable amount of P(LLA)$_{49}$ homopolymer to match the PLLA content of samples shown in Figure 7a) (Figure S24). In all cases, the blends proved to be less tough and less elastic than samples with more PLLA integrated to the polymer graft. We can thus conclude that the mechanical properties of our graft are the results of the successful grafting of PLLA on the P(γMCL) backbone with only low levels of un-grafted PLLA.

Also, the blends of the graft copolymers and free PLLA described above are hazy (Figure S25). One of the drawbacks of using semi-crystalline PLLA, in materials, can be its lack of

transparency. Our copolymers, however, are transparent, even with very high PLLA content (Figure 9).

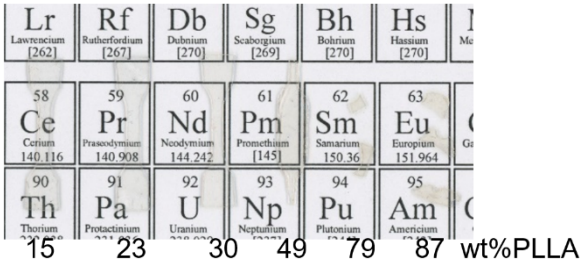

Figure 9. Image of P(γMCL)-*g*-PLLA with various PLLA content.

Finally, copolymers with the same PLLA content (30 wt%), same backbone length but different graft density and graft length were studied (Figure 7c)). The graft density seemed critical to obtain tough and elastic materials. A graft density of 0.6 % (with PLLA grafts of 7 kg/mol) appeared to give the best tensile properties. Higher grafting density of 1.5 % (due to smaller PLLA grafts of 3 kg/mol), resulted in properties close to those observed for graft copolymers with 15 wt% PLLA and 0.2 % for the graft density, i.e., strain at break above 1600 % but a stress at break below 8 MPa. This trend supports the claims shown in Figure 7b, where the longer the graft, the higher the stress at break. A lower graft density, 0.2 %, gave low strains at break and stresses at break.

Conclusions

We have developed the efficient one-pot synthesis of a new biobased macromonomer, a lactone-terminated PLLA. After optimizing the conditions, macromonomers of up to 14 kg/mol were synthesized using minimal solvent under 24 h. The complete conversion of the chain-ends was demonstrated through ^{1}H NMR and MALDI experiments. The optimized conditions for the grafting-through copolymerization of those macromonomers with γMCL were 100 °C and 2.5 M in toluene using DPP as the catalyst. Thermal analysis, DSC, and SAXS patterns showed that the graft copolymers are microphase separated. The strain-stress behaviors of various graft

copolymers were investigated. The backbone length proved to be of little importance for the mechanical properties above about 59 kg/mol. Grafting density, graft length and wt% of PLLA content all play a key role for tuning the graft copolymers properties. The materials properties can be tuned by changing the P(γMCL)/PLLA ratio. A grafting density higher than 0.6 % (and more than 2 graft/chains), was essential for robust elastomeric properties, thus ensuring enough bridging of P(γMCL) between distinct PLLA domains. Using a 7 kg/mol macromonomer is the best choice for a high stress at break and low residual strain. We report the first example of a fully biobased, aliphatic graft copolymer TPE with attractive elastomeric properties.

Associated content

Supporting information

NMR spectroscopy, MALDI-TOF spectrometry, size exclusion chromatography, tensile test, and X-ray scattering data.

Author information

Corresponding Author

*E-mail hillmyer@umn.edu

Acknowledgments

We thank Steven Weigand for the SAXS data collections. SAXS experiments were performed at the DuPont-Northwestern-Dow Collaborative Access Team (DND-CAT) located at the Sector 5 of the Advanced Photon Source (APS). DND-CAT is supported by E.I. DuPont de Nemours & Co., the Dow Chemical Company, and Northwestern University. Use of the APS, an Office of Science User Facility operated for the U.S. DOE Office of Science by Argonne National Laboratory, was supported by the U.S. DOE under contract no. DE-AC02-

06CH11357. We thank Christopher A. DeRosa and Huiqun Wang for helpful discussion and critical evaluation. We thank Marianne S. Meyersohn and Stephanie Liffland for their critical evaluation. Financial support for this work was provided by the Minnesota Corn Growers' Association. We also acknowledge the Center for Sustainable Polymers at the University of Minnesota, a National Science Foundation supported center for Chemical Innovation (CHE-1901635).

References

(1) Plastic - the facts, *Plastic Europe*, **2020**.
(2) Chinthapalli, R.; Skoczinski, P.; Carus, M.; Baltus, W.; de Guzman, D.; Käb, H.; Raschka, A.; Ravenstijn, J. Biobased Building Blocks and Polymers—Global Capacities, Production and Trends, 2018–2023. *Ind. Biotechnol.* **2019**, *15*, 237–241.
(3) Anastas, P. T.; Warner, J. C. *Oxford University Press: New York*, **1998**, p.30.
(4) Anastas, P. T.; Zimmerman, J. B. The Periodic Table of the Elements of Green and Sustainable Chemistry. *Green Chem.* **2019**, *21*, 6545–6566.
(5) Drobny, J. G. Handbook of Thermoplastic Elastomers, *William Andrew Publishing, New York,* **2007**.
(6) Holden, G.; Kricheldorf, H. R.; Quirk, R. P. Thermoplastic Elastomers, 3rd ed. *Hanser Gardner Publications, Inc.: Cincinnati,* **2004**.
(7) Duan, Y.; Thunga, M.; Schlegel, R.; Schneider, K.; Rettler, E.; Weidisch, R.; Siesler, H. W.; Stamm, M.; Mays, J. W.; Hadjichristidis, N. Morphology and Deformation Mechanisms and Tensile Properties of Tetrafunctional Multigraft Copolymers. *Macromolecules* **2009**, *42*, 4155–4164.
(8) Hadjichristidis, N.; Pitsikalis, M.; Iatrou, H.; Pispas, S. The Strength of the Macromonomer Strategy for Complex Macromolecular Architecture: Molecular Characterization, Properties and Applications of Polymacromonomers. *Macromol. Rapid Commun.* **2003**, *24*, 979–1013.
(9) Keith, A. N.; Clair, C.; Lallam, A.; Bersenev, E. A.; Ivanov, D. A.; Tian, Y.; Dobrynin, A. V.; Sheiko, S. S. Independently Tuning Elastomer Softness and Firmness by Incorporating Side Chain Mixtures into Bottlebrush Network Strands. *Macromolecules* **2020**, *53*, 9306–9312.
(10) Kawamoto, K.; Zhong, M.; Gadelrab, K. R.; Cheng, L.-C.; Ross, C. A.; Alexander-Katz, A.; Johnson, J. A. Graft-through Synthesis and Assembly of Janus Bottlebrush Polymers from A- *Branch* -B Diblock Macromonomers. *J. Am. Chem. Soc.* **2016**, *138*, 11501–11504.
(11) Vohidov, F.; Milling, L. E.; Chen, Q.; Zhang, W.; Bhagchandani, S.; Nguyen, H. V.-T.; Irvine, D. J.; Johnson, J. A. ABC Triblock Bottlebrush Copolymer-Based Injectable Hydrogels: Design, Synthesis, and Application to Expanding the Therapeutic Index of Cancer Immunochemotherapy. *Chem. Sci.* **2020**, 11, 5974-5986.
(12) Hilf, S.; Kilbinger, A. F. M. An All-ROMP Route to Graft Copolymers. *Macromol. Rapid Commun.* **2007**, *28*, 1225–1230.
(13) Mecerreyes, D.; Atthoff, B.; Boduch, K. A.; Trollsås, M.; Hedrick, J. L. Unimolecular Combination of an Atom Transfer Radical Polymerization Initiator and a Lactone Monomer as a Route to New Graft Copolymers. *Macromolecules* **1999**, *32*, 5175–5182.
(14) Rieger, J.; Bernaerts, K. V.; Du Prez, F. E.; Jérôme, R.; Jérôme, C. Lactone End-Capped Poly(Ethylene Oxide) as a New Building Block for Biomaterials. *Macromolecules* **2004**, *37*, 9738–9745.
(15) Maharana, T.; Mohanty, B.; Negi, Y. S. Melt–Solid Polycondensation of Lactic Acid and Its Biodegradability. *Prog. Polym. Sci.* **2009**, *34*, 99–124.
(16) Corneillie, S.; Smet, M. PLA Architectures: The Role of Branching. *Polym. Chem.* **2015**, *6*, 850–867.
(17) Leng, X.; Wei, Z.; Ren, Y.; Li, Y.; Wang, Y.; Wang, Q. Facile Synthesis and Comparative Study of Poly(L -Lactide) with Linear-Comb and Star-Comb Architecture. *RSC Adv.* **2015**, *5*, 81482–81491.

(18) Leng, X.; Wei, Z.; Bian, Y.; Ren, Y.; Wang, Y.; Wang, Q.; Li, Y. Rheological Properties and Crystallization Behavior of Comb-like Graft Poly(L -Lactide): Influences of Graft Length and Graft Density. *RSC Adv.* **2016**, *6*, 30320–30329.
(19) Zhu, Y.; Akagi, T.; Akashi, M. Preparation and Characterization of Nanoparticles Formed through Stereocomplexation between Enantiomeric Poly(γ-Glutamic Acid)-Graft-Poly(Lactide) Copolymers. *Polym. J.* **2013**, *45*, 560–566.
(20) Ishimoto, K.; Arimoto, M.; Okuda, T.; Yamaguchi, S.; Aso, Y.; Ohara, H.; Kobayashi, S.; Ishii, M.; Morita, K.; Yamashita, H.; Yabuuchi, N. Biobased Polymers: Synthesis of Graft Copolymers and Comb Polymers Using Lactic Acid Macromonomer and Properties of the Product Polymers. *Biomacromolecules* **2012**, *13*, 3757–3768.
(21) Leng, X.; Zhang, W.; Wang, Y.; Wang, Y.; Li, X.; Wei, Z.; Li, Y. Hydrolytic Degradation of Comb-Like Graft Poly (Lactide-Co-Trimethylene Carbonate): The Role of Comonomer Compositions and Sequences. *Polymers* **2019**, *11*, 2024.
(22) Zhang, J.; Schneiderman, D. K.; Li, T.; Hillmyer, M. A.; Bates, F. S. Design of Graft Block Polymer Thermoplastics. *Macromolecules* **2016**, *49*, 9108–9118.
(23) Haugan, I. N.; Lee, B.; Maher, M. J.; Zografos, A.; Schibur, H. J.; Jones, S. D.; Hillmyer, M. A.; Bates, F. S. Physical Aging of Polylactide-Based Graft Block Polymers. *Macromolecules* **2019**, *52*, 8878–8894.
(24) Kang, Y.; Wang, C.; Shi, X.; Zhang, G.; Chen, P.; Wang, J. Crystallization, Rheology Behavior, and Antibacterial Application of Graphene Oxide- Graft -Poly (l -Lactide)/Poly (l -Lactide) Nanocomposites. *Appl. Surf. Sci.* **2018**, *451*, 315–324.
(25) Yang, L.; Zhen, W. Preparation and Characterization of Phosphorylated Graphene Oxide Grafted with Poly(L-lactide) and Its Effect on the Crystallization, Rheological Behavior, and Performance of Poly (Lactic Acid). *Polym. Adv. Technol.* **2019**, *30*, 2846–2859.
(26) Chile, L.-E.; Kaser, S. J.; Hatzikiriakos, S. G.; Mehrkhodavandi, P. Synthesis and Thermorheological Analysis of Biobased Lignin-Graf t- Poly(Lactide) Copolymers and Their Blends. *ACS Sustainable Chem. Eng.* **2018**, *6*, 1650−1661.
(27) Pal, A. K.; Bhattacharjee, S. K.; Gaur, S. S.; Pal, A.; Katiyar, V. Chemomechanical, Morphological, and Rheological Studies of Chitosan- *Graft* -Lactic Acid Oligomer Reinforced Poly(Lactic Acid) Bionanocomposite Films. *J. Appl. Polym. Sci.* **2018**, *135*, 45546.
(28) Kaliva, M.; Georgopoulou, A.; Dragatogiannis, D. A.; Charitidis, C. A.; Chatzinikolaidou, M.; Vamvakaki, M. Biodegradable Chitosan-Graft-Poly(l-Lactide) Copolymers For Bone Tissue Engineering. *Polymers* **2020**, *12*, 316.
(29) Kim, J. Y.; Ha, C. S.; Jo, N. J. Synthesis and Properties of Biodegradable Chitin-Graft-Poly(L-Lactide) Copolymers. *Polym. Int.* **2002**, *51*, 1123–1128.
(30) Chuensangjun, C.; Kanomata, K.; Kitaoka, T.; Chisti, Y.; Sirisansaneeyakul, S. Surface-Modified Cellulose Nanofibers-Graft-Poly(Lactic Acid)s Made by Ring-Opening Polymerization of l-Lactide. *J. Polym. Environ.* **2019**, *27*, 847–861.
(31) Bao, J.; Han, L.; Shan, G.; Bao, Y.; Pan, P. Preferential Stereocomplex Crystallization in Enantiomeric Blends of Cellulose Acetate- *g* -Poly(Lactic Acid)s with Comblike Topology. *J. Phys. Chem. B* **2015**, *119*, 12689–12698.
(32) Volokhova, A. S.; Waugh, J. B.; Arrington, K. J.; Matson, J. B. Effects of Graft Polymer Compatibilizers in Blends of Cellulose Triacetate and Poly(Lactic Acid). *Polym. Int.* **2019**, *68* (7), 1263–1270.
(33) Zhang, P.; She, P.; He, J.; Xiang, Z.; Li, Z.; Cao, Y.; Zhang, X. Full-Biodegradable Polylactide-Based Thermoresponsive Copolymer with a Wide Temperature Range: Synthesis, Characterization and Thermoresponsive Properties. *React. Funct. Polym.* **2019**, *142*, 128–133.

(34) Zhou, C.; Wei, Z.; Jin, C.; Wang, Y.; Yu, Y.; Leng, X.; Li, Y. Fully Biobased Thermoplastic Elastomers: Synthesis of Highly Branched Linear Comb Poly(β-Myrcene)-Graft-Poly(l-Lactide) Copolymers with Tunable Mechanical Properties. *Polymer* **2018**, *138*, 57–64.
(35) Wahlen, C.; Rauschenbach, M.; Blankenburg, J.; Kersten, E.; Ender, C. P.; Frey, H. Myrcenol-Based Monomer for Carbanionic Polymerization: Functional Copolymers with Myrcene and Bio-Based Graft Copolymers. *Macromolecules* **2020**, *53*, 9008–9017.
(36) Watts, A.; Kurokawa, N.; Hillmyer, M. A. Strong, Resilient, and Sustainable Aliphatic Polyester Thermoplastic Elastomers. *Biomacromolecules* **2017**, *18*, 1845–1854.
(37) Liffland, S.; Hillmyer, M. A. *Macromolecules* **2021**, *54*, 9327–9340.
(38) Lundberg, D. J.; Lundberg, D. J.; Hillmyer, M. A.; Dauenhauer, P. J. Techno-Economic Analysis of a Chemical Process To Manufacture Methyl-ε-Caprolactone from Cresols. *ACS Sustain. Chem. Eng.* **2018**, *6*, 15316–15324.
(39) Reisman, L.; Siehr, A.; Horn, J.; Batiste, D. C.; Kim, H. J.; De Hoe, G. X.; Ellison, C. J.; Shen, W.; White, E. M.; Hillmyer, M. A. Respirometry and Cell Viability Studies for Sustainable Polyesters and Their Hydrolysis Products. *ACS Sustain. Chem. Eng.* **2021**, *9*, 2736–2744.
(40) Lohmeijer, B. G. G.; Pratt, R. C.; Leibfarth, F.; Logan, J. W.; Long, D. A.; Dove, A. P.; Nederberg, F.; Choi, J.; Wade, C.; Waymouth, R. M.; Hedrick, J. L. Guanidine and Amidine Organocatalysts for Ring-Opening Polymerization of Cyclic Esters. *Macromolecules* **2006**, *39*, 8574–8583.
(41) _Efforts were put to replace mCPBA by oxone, but this approach was not efficacious. Procedures were inspired from references 42 to 45.
(42) Chrobok, A. The Baeyer–Villiger Oxidation of Ketones with Oxone® in the Presence of Ionic Liquids as Solvents. *Tetrahedron* **2010**, *66*, 6212–6216.
(43) Martello, M. T.; Hillmyer, M. A. Polylactide–Poly(6-Methyl-ε-Caprolactone)–Polylactide Thermoplastic Elastomers. *Macromolecules* **2011**, *44*, 8537–8545.
(44) Baj, S.; Chrobok, A.; Siewniak, A. New and Efficient Technique for the Synthesis of Ɛ-Caprolactone Using KHSO5 as an Oxidising Agent in the Presence of a Phase Transfer Catalyst. *Appl. Catal. A-Gen.* **2011**, *395*, 49–52.
(45) Disetti, P.; Piras, L.; Moccia, M.; Saviano, M.; Adamo, M. F. A. Model Studies for the Preparation of Oxepanes and Fused Compounds by Tandem [4+3] Cycloaddition/Ring-Opening Metathesis/Cross Metathesis: Model Studies for the Preparation of Oxepanes and Fused Compounds by Tandem [4+3] Cycloaddition/Ring-Opening Metathesis/Cross Metathesis. *Eur. J. Org. Chem.* **2017**, *2017*, 6202–6208.
(46) Mezzasalma, L.; Dove, A. P.; Coulembier, O. Organocatalytic Ring-Opening Polymerization of l-Lactide in Bulk: A Long Standing Challenge. *Eur. Polym. J.* **2017**, *95*, 628–634.
(47) Prat, D.; Wells, A.; Hayler, J.; Sneddon, H.; McElroy, C. R.; Abou-Shehada, S.; Dunn, P. J. CHEM21 Selection Guide of Classical- and Less Classical-Solvents. *Green. Chem.* **2016**, *18*, 288-296.
(48) Vaida, C.; Takwa, M.; Martinelle, M.; Hult, K.; Keul, H.; Möller, M. γ -Acyloxy- ε -Caprolactones: Synthesis, Ring-Opening Polymerization vs. Rearrangement by Means of Chemical and Enzymatic Catalysis. *Macromol. Symp.* **2008**, *272*, 28–38.
(49) Batiste, D. C.; Meyersohn, M. S.; Watts, A.; Hillmyer, M. A. Efficient Polymerization of Methyl-ε-Caprolactone Mixtures To Access Sustainable Aliphatic Polyesters. *Macromolecules*, **2020**, *53*, 1795−1808.
(50) Makiguchi, K.; Kikuchi, S.; Yanai, K.; Ogasawara, Y.; Sato, S.; Satoh, T.; Kakuchi, T. Diphenyl Phosphate/4-Dimethylaminopyridine as an Efficient Binary Organocatalyst

System for Controlled/Living Ring-Opening Polymerization of L -Lactide Leading to Diblock and End-Functionalized Poly(L-Lactide)s. *J. Polym. Sci. Part Polym. Chem.* **2014**, *52*, 1047–1054.
(51) Beckingham, B. S.; Sanoja, G. E.; Lynd, N. A. Simple and Accurate Determination of Reactivity Ratios Using a Nonterminal Model of Chain Copolymerization. *Macromolecules* **2015**, *48*, 6922–6930.
(52) Bhattarai, N.; Khil, M. S.; Oh, S. J.; Kim, H. Y.; Kim, K. W. Thermal Decomposition Kinetics of Copolymers Derived Fromp-Dioxanone, L-Lactide and Poly(Ethylene Glycol). *Fibers Polym.* **2004**, *5*, 289–296.
(53) Jamshidi, K.; Hyon, S.-H.; Ikada, Y. Thermal Characterization of Polylactides. *Polymer* **1988**, *29*, 2229–2234.
(54) Fan, Y.; Nishida, H.; Shirai, Y.; Endo, T. Thermal Stability of Poly (l-Lactide): Influence of End Protection by Acetyl Group. *Polym. Degrad. Stab.* **2004**, *84*, 143–149.
(55) Using a reference volume of 118 Å3: Wu, L.; Cochran, E. W.; Lodge, T. P.; Bates, F. S. Consequences of Block Number on the Order−Disorder Transition and Viscoelastic Properties of Linear (AB) $_n$ Multiblock Copolymers. *Macromolecules* **2004**, *37*, 3360–3368.
(56) Olvera de la Cruz, M.; Sanchez, I. C. Theory of microphase separation in graft and star copolymers. *Macromolecules* **1986**, *19*, 2501–2508.
(57) Chu, B.; Hsiao, B. S. Small-Angle X-Ray Scattering of Polymers. *Chem. Rev.* **2001**, *101*, 1727–1762.
(58) Tong, J.-D.; Jerôme, R. Dependence of the Ultimate Tensile Strength of Thermoplastic Elastomers of the Triblock Type on the Molecular Weight between Chain Entanglements of the Central Block. *Macromolecules* **2000**, *33*, 1479–1481.